Journal of Power Sources 190 (2009) 210–215

Contents lists available at ScienceDirect

Journal of Power Sources

journal homepage: www.elsevier.com/locate/jpowsour

Ultrasonic synthesis and evaluation of non-platinum catalysts for alkaline direct methanol fuel cells

Hideaki Bunazawa, Yohtaro Yamazaki*

Department of Innovative and Engineered Materials, Interdisciplinary Graduate School of Science and Engineering, Tokyo Institute of Technology, 4259 Nagatsuta-cho, Midori-ku, Yokohama, Kanagawa 226-8502, Japan

ARTICLE INFO

Article history:
Received 25 November 2008
Received in revised form 21 January 2009
Accepted 27 January 2009
Available online 6 February 2009

Keywords:
Fuel cell
DMFC
Alkaline
Anion
Ultrasonic
Cavitation

ABSTRACT

Ultrasonic synthesis was investigated as a synthesis method of non-platinum catalysts for alkaline direct methanol fuel cells (alkaline DMFCs) such as 20% mass Pd/C, Au/C, and PdAu/C. Among four kinds of solvents, ethylene glycol was demonstrated to be the optimum solvent for the synthesis of those catalysts. When ethylene glycol was used, the synthesized metal nanoparticles were highly dispersed on carbon particles. The synthesized Pd/C and PdAu/C showed the high oxygen reduction reaction (ORR) activity in alkaline condition (0.5 M NaOH aqueous solution), which was comparable to conventional Pt/C. Moreover, they showed lower methanol oxidation reaction (MOR) activity. Membrane electrode assemblies (MEAs) containing the synthesized Pd/C cathode catalysts and alkaline ion exchange membranes were fabricated and evaluated by single cell tests. They showed high performance that was comparable to MEAs with Pt/C cathode. In addition, it was found that the synthesized Pd/C was relatively tolerant to methanol crossover.

1. Introduction

Recently, the research on alkaline direct methanol fuel cells (alkaline DMFCs) using alkaline ion (OH^-) exchange membranes has been increasing [1,2]. Unlike conventional DMFCs using proton (H^+) exchange membrane, alkaline DMFCs allow for the use of inexpensive non-platinum metal catalysts such as silver and nickel. In addition, the overvoltage in alkaline DMFCs was restricted by the faster kinetics of electrode reactions and lower methanol permeability.

Until now, many structural and electrochemical studies on alkaline DMFCs have been done [3]. The synthesis and evaluation of many kinds of alkaline ion exchange membranes have been reported [4–7]. Most of the alkaline ion exchange membranes have a polymer structure that contains quaternary ammonium groups conducting OH^- ions. Recently, the mechanism of membrane degradation is also investigated [8,9]. These results suggested that the chemical and thermal stability of alkaline ion exchange membranes are not high enough compared with conventional proton exchange membranes. In addition to the study on electrolytes, feasibility of the anode fuels is investigated. It is reported that ethylene glycol [10], hydrazine [11], sodium hydride [12], and the other fuels are available. Nevertheless, most of the fuels are blended with KOH (NaOH) in order to observe high performance [13]. This is not suitable for the practical use because KOH possibly induce some problems.

On the other hand, there are still few reports about non-platinum metal catalysts for alkaline DMFCs [14,15] even though non-platinum catalysts are one of the most attractive advantages of alkaline DMFCs. Non-platinum catalysts such as Au/C, Ag/C are investigated as alternatives to Pt-type catalysts, but their electrocatalytic activity is shown to be much lower than Pt-type catalysts. Therefore, the study on high performance non-platinum catalysts is necessary for the development of alkaline DMFCs.

It is well known that the ultrasonic synthesis is an attractive method for synthesizing transition metal nanoparticles, especially for noble metal (Pt, Pd, Au, and Ag) nanoparticles [16–19]. Up to now, there are many reports that succeed in ultrasonically synthesizing Pd, Au and the other metal nanoparticles under 10 nm. The ultrasonic synthesis is also used for preparing metal nanoparticles supported on indium doped tin oxide (ITO) and maghemite [20,21]. Therefore, in this study, ultrasonic synthesis is investigated for preparing non-platinum catalysts such as Pd, Au and PdAu supported on carbon particles, and electrochemical tests of these catalysts were conducted.

* Corresponding author. Tel.: +81 45 924 5411; fax: +81 45 924 5411.
E-mail addresses: bunazawa.h.aa@m.titech.ac.jp (H. Bunazawa), yamazaki.y.af@m.titech.ac.jp (Y. Yamazaki).

0378-7753/$ – see front matter © 2009 Elsevier B.V. All rights reserved.
doi:10.1016/j.jpowsour.2009.01.077

2. Experimental

2.1. Synthesis of 20% mass Pd/C, Au/C, and PdAu/C

The preparation of 20% mass Pd/C, Au/C, and PdAu (1:1)/C catalysts was carried out by means of ultrasonic synthesis. First of all, metal precursor and surfactant were dissolved in solvents. As palladium and gold metal precursors, ammonium tetrachloropalladate ($(NH_4)_2PdCl_4$, 97%, Aldrich) and gold chloride trihydrate ($HAuCl_4{\cdot}3H_2O$, >99.9%, Aldrich) were used, respectively. As a surfactant, citric acid (Wako) was used. The molar ratio of metal to surfactant was 1–21. Second, 0.0838 g Vulcan XC72 (Cabot) used as a carbon support was dispersed into the above solution. The prepared mixture was placed in an ice bath, and purged with argon to eliminate the oxygen in it. Finally, the mixture was sonicated by means of an ultrasonic homogenizer (VP-15S, TAITEC). Ultrasonic irradiation was operated at 20 kHz, with an input power of 105 W. The experimental setup is schematically shown in Fig. 1. In order to characterize, the prepared catalysts were separated by centrifuging at 4000 rpm, and washed with distilled water and ethanol repeatedly. Then, they were dried in vacuum at 80 °C.

2.2. Characterization

The shape and size of the prepared catalysts were investigated using a transmission electron microscope (TEM, Hitachi H-8100, operating at 200 kHz). The samples for TEM observation were prepared by placing a drop of the catalyst suspension in ethanol onto a carbon coated copper grid, followed by natural evaporation of the solvent at room temperature. In addition, X-ray diffraction (XRD) measurements of catalysts were performed using a Rigaku RINT 2000 diffractrometer with Cu Kα target at 40 kV and 40 mA. The diffraction angle ranged from 10° to 90° with a scan rate of $2^\circ\ min^{-1}$.

In order to evaluate the redox activity of the prepared catalysts for H_2, O_2, and MeOH in alkaline condition, cyclic voltammetry (CV) was conducted with a conventional three-electrode configuration at 25 °C. The working electrode was fabricated by the following procedure. The prepared catalyst was put on a glassy carbon electrode (diameter: 5 mm) by placing a drop of 15 μl catalyst suspension.

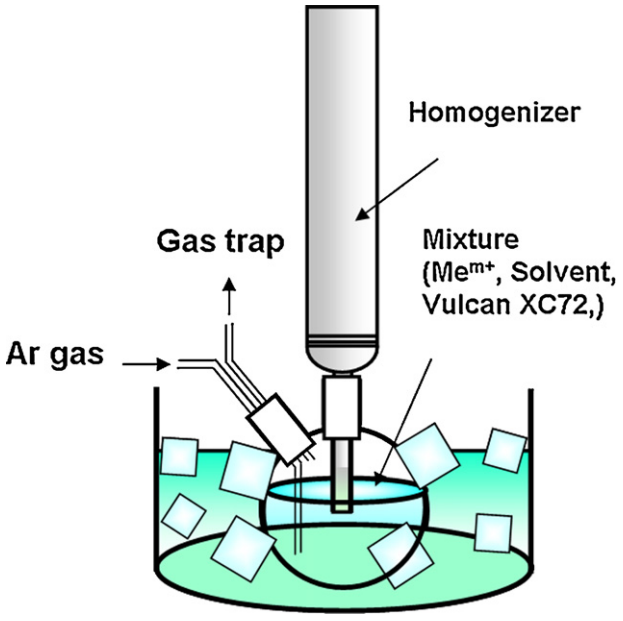

Fig. 1. Schematic diagram of ultrasonic synthesis.

The catalyst suspension was prepared by dispersing 5 mg prepared catalyst in 1 ml distilled water (Millipore MilliQ 18 MΩ cm) using an ultrasonic bath. After dried at room temperature for 30 min and in vacuum at 80 °C for 10 min, they were coated with an anion ionomer. Anion ionomer solution (0.784 μl, 5% mass A3-solution, Tokuyama, diluted to 0.324% mass) was dropped on them, followed by drying at room temperature for 15 min, in vacuum at 80 °C for 10 min. Pt coil and Ag/AgCl (sat. KCl, +0.199 V vs. SHE) electrode were used as the counter and the reference electrodes, respectively. NaOH (0.5 M) aqueous solution saturated with O_2 or NaOH (0.5 M) aqueous solution with MeOH (0.1 M) purged with Ar were used as the electrolyte. CV measurement was operated and recorded by an HZ3000 (Hokuto Denko).

2.3. Fabrication of membrane electrode assembly

MEAs with an active area of 1 cm^2 were fabricated by the dry spraying method [22,23]. Prior to the electrode coating, anion exchange membranes (A201, thickness: 28 μm, Tokuyama) and carbon papers (TGP-H-060, thickness: 190 μm, containing microporous layer, TORAY) were cut into 3 cm × 3 cm and 1 cm × 1 cm, respectively. The anode electrodes were coated as follows. The catalyst ink for six MEAs was prepared by blending 0.124 g PtRu/C (30% mass Pt, 23.3% mass Ru, Vulcan XC72, Tanaka Kikinzoku), 0.67 g distilled water, 1.03 g anion ionomer (5% mass A3-solution, Tokuyama), and 1.2 g 1-propanol. The prepared catalyst ink was sprayed onto both the anion exchange membranes and carbon papers by a spray gun. The anion exchange membranes were masked and only 1 cm × 1 cm was exposed. Untreated carbon papers were used as the anode gas diffusion layer (GDLs). After dried for 1 day in ambient condition, cathode electrode containing the synthesized 20% mass Pd/C or purchased Pt/C (19.8% mass, Vulcan XC72, Tanaka Kikinzoku) was coated similarly. Hydrophobic carbon papers were used as the cathode GDLs. For the hydrophobic GDLs, the carbon papers were treated by calcinations at 400 °C for 1 h after immersing in 15% mass PTFE suspension. The anion exchange membrane and carbon papers were physically assembled by cell fixture without hot pressing because the thermal stability of anion exchange membrane was low.

2.4. Fuel cell testing

The fuel cell testing was conducted as the following condition. The fabricated MEA was mounted in a single cell test fixture (Electrochem) containing graphite blocks with serpentine flow channels and current collector plates. Prior to the fuel cell testing, the cell temperature was held at 80 °C, and the anode and cathode flow channels were purged with distilled water (5.0 ml min^{-1}, preheated at 80 °C) and N_2 gas (100 ml min^{-1}, humidified at 80 °C), respectively. After that, MeOH (0.2, 0.5, 1, 2, 3, and 5 M) aqueous solution (5.0 ml min^{-1}, preheated at 80 °C) and O_2 gas (100 ml min^{-1}, humidified at 80 °C) were supplied to the anode and cathode, respectively. The fuel cell test was conducted by periodically recording *I–V* curve (25 mV $point^{-1}$ from OCV, 1 min $point^{-1}$) after keeping at OCV for 30 min.

3. Results and discussion

3.1. Solvent effect

Non-platinum catalysts consisting of metal nanoparticles supported on high active area carbon supports (Vulcan XC72) were produced by means of ultrasonic synthesis. The origin of the ultrasonic synthesis is acoustic cavitation: the formation, growth, and implosive collapse of gas cavities within a liquid. The implosive

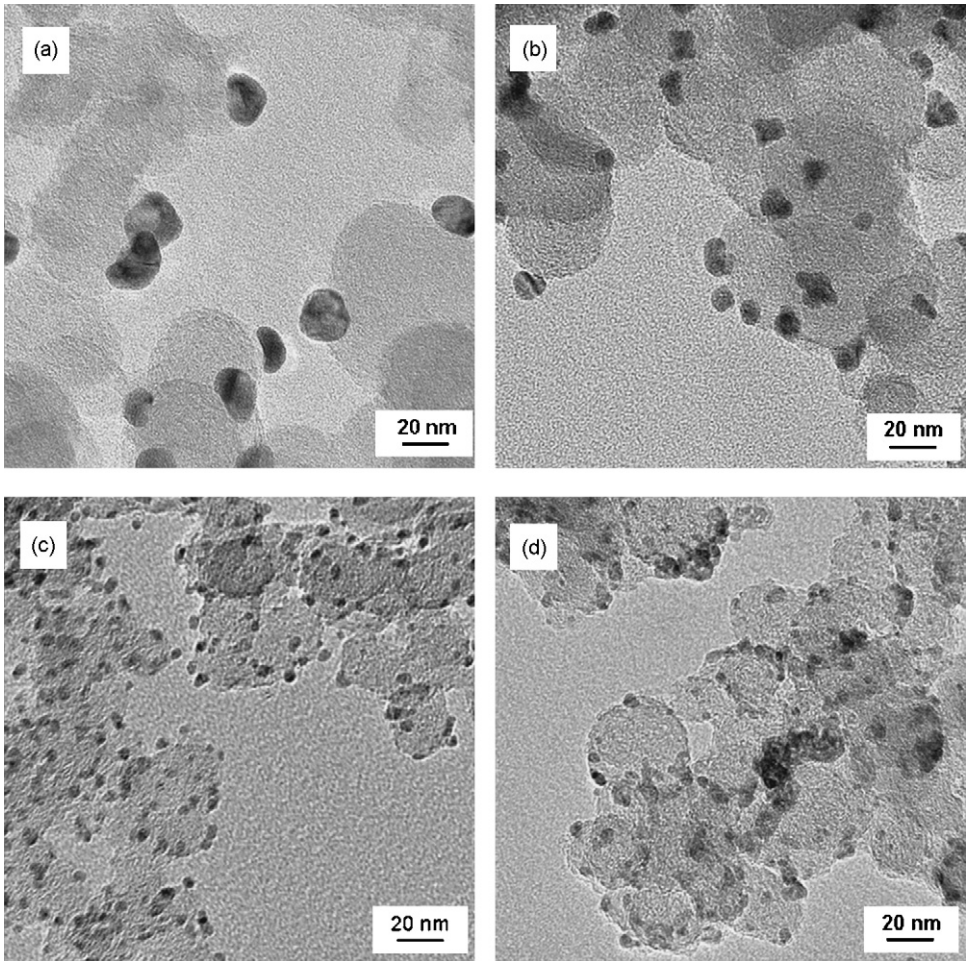

Fig. 2. TEM images of 20% mass Pd/C synthesized in (a) distilled water, (b) ethanol, (c) ethylene glycol, and (d) tetraethylene glycol; ultrasonic condition: 20 kHz, 105 W.

collapse of gas cavities is induced on the surface of carbon particles. As a result, high temperature and high pressure reaction sites (~5000 K, ~2000 atm) are locally generated, and H•, OH•, and the other radical species that can reduce metal ions were produced. The reduction reaction mechanism of the ultrasonic synthesis is shown below:

$$RH(ROH) \rightarrow R^{\bullet} + H^{\bullet}(OH^{\bullet})$$

$$H^{\bullet}(OH^{\bullet}) + RH \rightarrow R^{\bullet} + H_2(H_2O)$$

$$M^{m+} + R_1{}^{\bullet} \rightarrow M^{(m-1)+} + R_2 + H^{+}$$

(R: solvent or surfactant, M: metal)

It is clear that the solvent plays an important role in the ultrasonic synthesis. Solvents produce the H•, OH•, and the other radicals that are essential for the reduction of metal ions. In addition, solvent properties such as vapor pressure and surface tension affect the condition of metal nanoparticles preparation because the formation of the reaction sites is influenced by these properties. Threshold pressure (P_{cc}) for the generation of acoustic cavitation is shown by the following formula [24]:

$$P_{cc} = P_0 - P_s + \left(\frac{16\pi Y_{LV}^3}{3kT \ln vA}\right)^{1/2}$$

where P_0 and P_s are the hydrostatic pressure and solvent's vapor pressure, Y_{LV} is the solvent's surface tension, k is the Boltzmann constant, T is the temperature and vA is the constant (=10^{25}). In addition to the above properties, polarity may be important to synthesize highly dispersed metal nanoparticles on the carbon support because it related to the Van der Waal's force between nanoparticles. Therefore, in this study, the solvent effects on Pd/C catalysts synthesis were firstly investigated.

Fig. 2 shows TEM images of the 20% mass Pd/C catalysts synthesized in various solvents (distilled water, ethanol, ethylene glycol (EG), and tetraethylene glycol (TEG)). Pd^{2+} was reduced by the acoustic cavitation nearby the carbon particles, and Pd nanoparticles were synthesized and supported on the carbon particles. The ultrasonic irradiation time of each sample was optimized between 5 and 10 min because the rates of Pd^{2+} reduction depended on the solvent. Fig. 2(a) shows Pd/C synthesized in distilled water for 5 min. The prepared Pd nanoparticles were supported on the carbon particles locally, and their size was large. One of the reasons for the Pd agglomeration was probably the hydrophobicity of the surface of carbon black. The carbon particles were not well dispersed in the distilled water during the ultrasonic irradiation, and there was little surface area that was available for supporting Pd nanoparticles. Fig. 2(b) and (d) shows Pd/C synthesized in ethanol for 10 min and TEG for 5 min, respectively. In these cases, the carbon particles were well dispersed in the solvents, and the prepared Pd nanoparticles were wholly supported on them. Nevertheless, the Pd agglomeration was observed as well. Fig. 2(c) shows Pd/C synthesized in EG for 5 min. Unlike other samples, the prepared Pd nanoparticles were very small, spherical in shape, and highly dispersed. Their size was not distributed. The average particle size of 3.6 and 3.4 nm was observed by TEM and XRD, respectively.

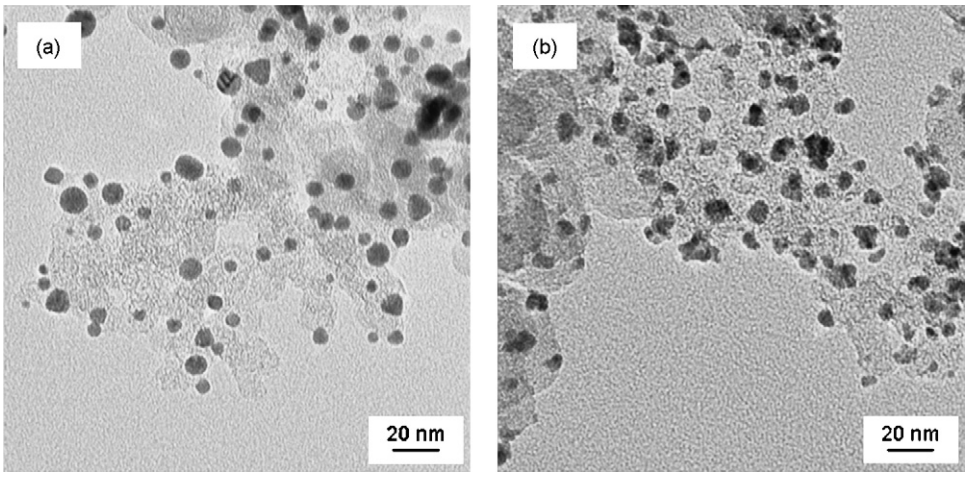

Fig. 3. TEM images of (a) 20% mass Au/C and (b) 20% mass PdAu/C; ultrasonic condition: 20 kHz, 105 W.

3.2. Ultrasonic synthesis of 20% mass Au/C and PdAu/C

According to previous researches, sonochemical reduction kinetics of Pd^{2+} and Au^{3+} were comparable. In this study, 20% mass Au/C and PdAu/C could be synthesized in EG as well as Pd/C. The optimized time of ultrasonic irradiation for Au/C and PdAu/C production was 5 and 7 min, respectively. Fig. 3 shows TEM images of the synthesized Au/C and PdAu/C. The synthesized Au and PdAu nanoparticles were highly dispersed on the carbon particles and the shape was sphere, especially for the Au nanoparticles. Comparing with the Pd nanoparticles, the size of the Au nanoparticles was larger and more distributed. The average Au particle size was distributed near 4.2 and 8.2 nm. The larger particle size indicated the rapid growth of Au nanoparticle. On the other hand, the size of the prepared PdAu nanoparticles was a little larger than the Pd nanoparticles, but PdAu nanoparticle size was not distributed like the Au nanoparticles. The average PdAu particle size of 4.8 and 4.5 nm were observed by TEM and XRD, respectively.

The result of XRD measurement is shown in Fig. 4. It is confirmed that the PdAu bimetallic catalysts were produced, and the crystal structure was face-centered cubic. The peaks of Pd/C and Au/C corresponded to the intrinsic peaks of Pd, Au and C. Furthermore, the peaks of PdAu/C were shifted between those of Pd/C and Au/C, which means that the synthesized PdAu/C was alloy catalyst. It has been demonstrated by other researchers that alloy catalysts have some unique electrochemical properties. Therefore, it was confirmed that ultrasonic synthesis was useful to synthesize electrocatalysts.

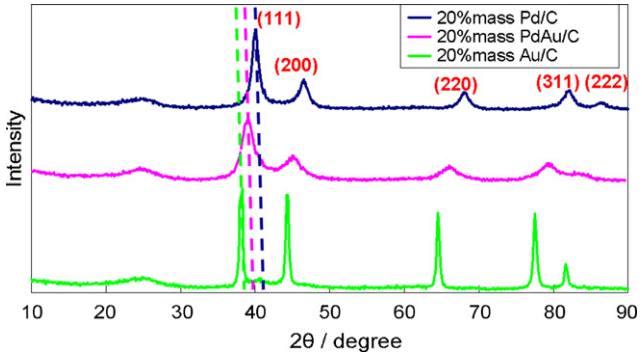

Fig. 4. XRD spectra of the synthesized 20% mass Pd/C, PdAu/C, and Au/C.

3.3. Cyclic voltammetry

The electrocatalytic activities of the synthesized catalysts in 0.5 M NaOH aqueous solution (in alkaline conditon) were evaluated by means of cyclic voltammetry. CV curves of commercialized 20% mass Pt/C (Tanaka Kikinzoku) was also measured as a reference. Fig. 5 shows the oxygen reduction reaction (ORR) activity of the catalysts after five potential cycles. Each CV curve started from around 1.0 V and reversed around 0.2 V. All the synthesized catalysts showed the ORR activity. The onset potential of the catalysts for the ORR was in the order Au/C < PdAu/C < Pd/C < Pt/C. The onset potential of the PdAu/C (0.990 V) and Pd/C (1.01 V) was almost the same, and a little more negative than that of the Pt/C (1.03 V). This result indicated that the ORR activity of the Pd/C and PdAu/C was comparable to that of the Pt/C. On the other hand, it was observed that the onset potential of the Au/C (0.823 V) was much more negative than the other catalysts. The ORR activity of the Au/C was confirmed to be lower than the other catalysts.

In addition to the ORR activity, the methanol oxidation reaction (MOR) activity of the catalysts was measured and compared. The CV measurement of the fifth cycle is shown in Fig. 6. Each CV curve started from around 0.2 V and reversed around 1.0 V. The synthesized Pd/C and PdAu/C showed the MOR activity, whereas the synthesized Au/C showed almost no MOR activity. The onset potential of the Pd/C and PdAu/C was 0.615 V and 0.630 V, which was about 0.15 V more positive than the Pt/C (0.465 V). In addition, it was shown that the peaks of the Pd/C and PdAu/C were much lower than the Pt/C. This result indicated that the MOR activity of

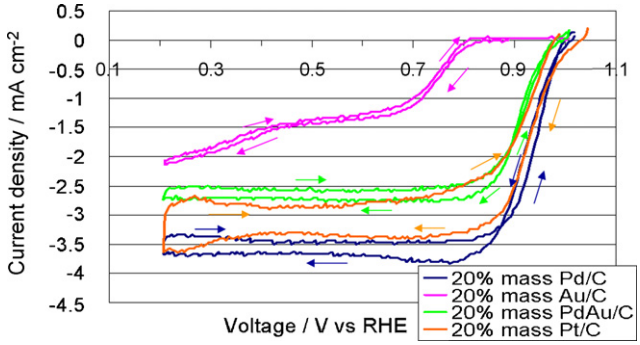

Fig. 5. Cyclic voltammogram of 20% mass Pd/C, Au/C, and PdAu/C at 25 °C; electrolyte: (0.5 M) NaOH aqueous solution saturated through O_2, working electrode: glassy carbon (1000 rpm), reference electrode: Ag/AgCl (+0.199 mV vs. SHE), scan rate: 10 mV s^{-1}.

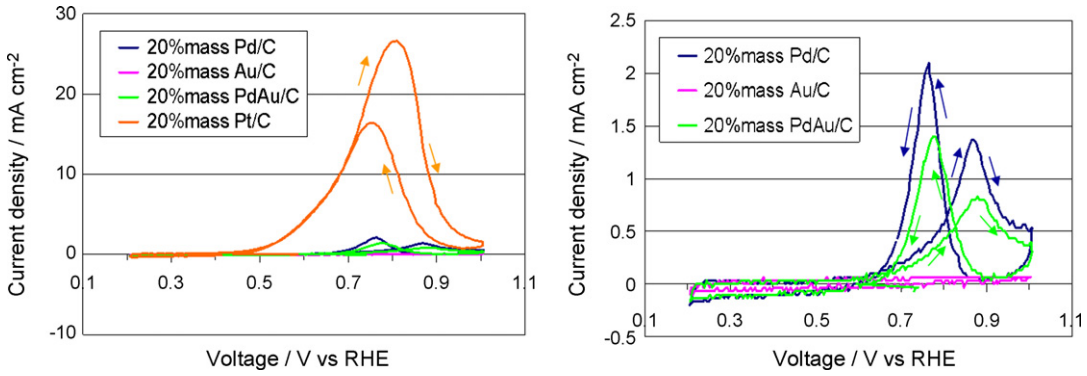

Fig. 6. Cyclic voltammogram of 20% mass Pd/C, Au/C, and PdAu/C at 25 °C; electrolyte: (0.5 M) NaOH aqueous solution blended with MeOH (0.1 M), working electrode: glassy carbon (1000 rpm), reference electrode: Ag/AgCl (+0.199 mV vs. SHE), scan rate: 10 mV s^{-1}.

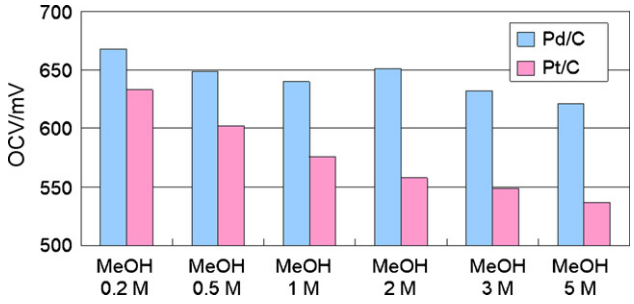

Fig. 7. Relation between OCV of MEAs and MeOH concentration at 80 °C; anode catalyst PtRu (Pt loading: 0.56 mg cm^{-2}, Ru loading 0.44 mg cm^{-2}), cathode catalyst Pd or Pt (loading: 0.50 mg cm^{-2}), anode fuel: MeOH (0.2, 0.5, 1, 2, 3, and 5 M, fuel flow rate: 5.0 ml min^{-1}), cathode gas: O_2 (100% RH) (O_2 flow rate: 100 ml min^{-1}).

the Pd/C and PdAu/C were lower than the Pt/C. Therefore, Pd/C and PdAu/C were shown to be unsuitable for anode reaction. However, they could be expected as a superior cathode catalyst because they were expected to prevent the potential loss caused by methanol crossover.

3.4. Fuel cell testing

MEAs were fabricated with the synthesized Pd/C cathode and evaluated by single cell test at 80 °C. MEAs with the commercialized Pt/C cathode were also evaluated as a reference. In order to evaluate the tolerance for methanol crossover, various concentrations of MeOH without KOH were used as the anode fuels.

Fig. 7 shows the comparison between MeOH concentration and the OCV of MEAs with Pd/C and Pt/C cathode. It was observed that the MEAs with Pd/C showed higher OCV than the MEAs with Pt/C at any MeOH concentration. The reason for the difference in OCV was the influence of methanol crossover. The Pd/C cathode voltage was expected to be less decreased by methanol crossover because the MOR activity of the Pd/C was lower than that of the Pt/C.

Fig. 7 also shows that the OCV was linearly decreased with the increase in MeOH concentration. This result corresponded to the fact that the MeOH permeation increases with the increase in MeOH concentration. In addition, it was observed that the ratio of OCV loss of MEAs with Pd/C was much lower than that of MEAs with Pt/C. When MeOH 0.2 M was used as the anode fuel, the OCV of MEAs with Pd/C and Pt/C were 668 and 633 mV, respectively. When MeOH 5 M was used, the OCV of MEAs with Pd/C and Pt/C were 621 and 537 mV, respectively. This result indicated that the Pd/C cathode was less sensitive to MeOH concentration than the Pt/C cathode. This trend was considered to be an attractive advantage of Pd/C cathode over Pt/C cathode.

In addition to the OCV measurement, Fig. 8(a) and (b) shows the *I–V* curves of MEAs with Pd/C and Pt/C, respectively. It was clearly observed that the performance of MEAs with Pd/C was not influenced by MeOH concentration, whereas that of MEAs with Pt/C was deeply influenced. The performance of MEAs with Pd/C was comparable to MEAs with Pt/C, and was not relatively decreased even when the high concentration MeOH (3–5 M) was used. When the low concentration (0.2–1 M) MeOH was used, the performance of MEAs with Pd/C was lower than that of MEAs with Pt/C. However, when the high concentration MeOH was used, the performance of MEAs with Pd/C was higher than that of MEAs with Pt/C. The performance of MEAs with Pt/C much decreased with further increase in MeOH concentration. When the high concentration MeOH was used, the performance of MEAs with Pt/C was much lower. The reason for the performance loss was that the activity of Pt/C was lowered due to methanol crossover. Consequently, it was found that Pd/C was promising alternative to Pt/C as cathode catalyst because it had not only high ORR activity but also high methanol tolerance.

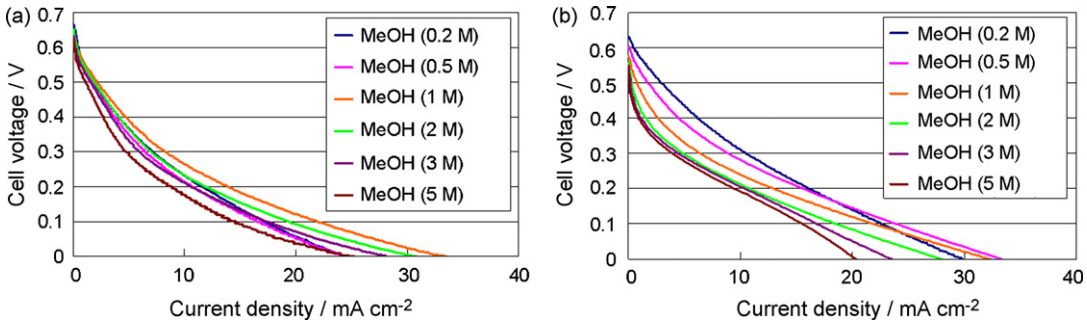

Fig. 8. *I–V* curves of MEAs with (a) Pd/C and (b) Pt/C cathode at 80 °C; anode catalyst PtRu (Pt loading: 0.56 mg cm^{-2}, Ru loading 0.44 mg cm^{-2}), cathode catalyst Pd or Pt (loading: 0.50 mg cm^{-2}), anode fuel: MeOH × M (0.2, 0.5, 1, 2, 3, and 5 M, fuel flow rate: 5.0 ml min^{-1}), cathode gas: humidified O_2 (O_2 flow rate: 100 ml min^{-1}), *I–V* measurement conditions: single test, 25 mV min^{-1} from OCV, 1 min $point^{-1}$.

4. Conclusion

20% mass Pd/C, Au/C and PdAu/C were synthesized by means of ultrasonic synthesis. The solvent effects on the synthesized Pd/C were clarified. The morphology of synthesized Pd/C such as particle size, distribution, and shape depended deeply on the properties of solvents. The synthesized metal nanoparticles were small and uniform in size, spherical in shape and highly dispersed on carbon black particles when ethylene glycol was used as solvent. It was observed by TEM that Au, and PdAu nanoparticles were also synthesized and highly dispersed on carbon support. The production of Pd/C, Au/C and PdAu/C were confirmed by XRD, and it was also revealed that the alloyed PdAu was synthesized. The electrochemical properties were measured by CV test. The synthesized Pd/C and PdAu/C showed a high ORR activity, which was comparable to Pt/C. On the other hand, the MOR activity of these catalysts was shown to be relatively low. The single cell test demonstrated the usefulness of the synthesized Pd/C as a cathode catalyst because MEAs with Pd/C cathode did not only show high performance, but also relatively high tolerance to methanol crossover.

References

[1] E.H. Yu, K. Scott, Electrochem. Commun. 6 (2004) 361–365.
[2] E.H. Yu, K. Scott, J. Power Sources 137 (2004) 248–256.
[3] E.H. Yu, K. Scott, J. Appl. Electrochem. 35 (2005) 91–95.
[4] J.-S. Park, G.-G. Park, S.-H. Park, Y.-G. Yoon, C.S. Kim, W.Y. Lee, Macromol. Symp. 249–250 (2007) 174–182.
[5] J.-S. Park, S.-H. Park, S.-D. Yim, Y.-G. Yoon, W.Y. Lee, C.S. Kim, J. Power Sources 178 (2008) 620–626.
[6] J. Fang, P. Kang, J. Membr. Sci. 285 (2006) 317–322.
[7] Y. Wan, B. Peppley, K.A.M. Creber, V. Tam Bui, E. Halliop, J. Power Sources 162 (2006) 105–113.
[8] S. Chempath, B.R. Einsla, L.R. Pratt, C.S. Macomber, J.M. Boncella, J.A. Rau, B.S. Pivovar, J. Phys. Chem. C 112 (2008) 3179–3182.
[9] J.R. Varcoe, R.C.T. Slade, Fuel Cells 5 (2005) 187–200.
[10] K. Matsuoka, Y. Iriyama, T. Abe, M. Matsuoka, Z. Ogumi, J. Power Sources 150 (2005) 27–31.
[11] K. Yamada, K. Yasuda, N. Fujiwara, Z. Siroma, H. Tanaka, Y. Miyazaki, T. Kobayashi, Electrochem. Commun. 5 (2003) 892–896.
[12] B.H. Liu, Z.P. Lo, K. Arai, S. Suda, Electrochem. Acta 50 (2005) 3719–3725.
[13] H. Bunazawa, Y. Yamazaki, J. Power Sources 182 (2008) 48–51.
[14] C. Coutanceau, L. Demarconnay, C. Lamy, J.-M. Léger, J. Power Sources 156 (2006) 14–19.
[15] J.R. Varcoe, R.C.T. Slade, G.L. Wright, Y. Chen, J. Phys. Chem. 110 (2006) 21041–21049.
[16] J.-E. Park, M. Atobe, T. Fuchigami, Electrochem. Acta 51 (2005) 849–854.
[17] Y. Mizukoshi, R. Oshima, Y. Yamada, Y. Nagata, Langmuir 15 (1999) 2733–2737.
[18] C. Kan, W. Cai, C. Li, L. Zhang, H. Hofmeister, J. Phys. D 36 (2003) 1609–1614.
[19] A. Nemamcha, J.-L. Rehspringer, D. Khatmi, J. Phys. Chem. B 110 (2006) 383–387.
[20] J.-E. Park, T. Momma, T. Osaka, Electrochem. Acta 52 (2007) 5914–5923.
[21] Y. Mizukoshi, Y. Tsuru, A. Tominaga, S. Seino, N. Masahashi, S. Tanabe, T. Yamamoto, Ultrason. Sonochem. 15 (2008) 875–880.
[22] E. Gűlzow, R. Reissner, S. Weisshaar, T. Kaz, Fuel Cells 3 (2003) 48–51.
[23] S.-J. Shin, J.-K. Lee, H.-Y. Ha, S.-A. Hong, H.-S. Chun, I.-H. Oh, J. Power Sources 106 (2002) 146–152.
[24] T. Matsunaga, K. Ogata, T. Hatayama, K. Shinozaki, M. Yoshida, J. Jpn. Inst. Light Mater. 56 (2006) 214–220.